



## Local Site Effects During the Orkney Earthquake of 5 August 2014

T. MULABISANA,<sup>1</sup> V. MIDZI,<sup>1</sup> and B. MANZUNZU<sup>1</sup>

**Abstract**—Site response analysis is conducted at 37 seismic stations located in the Gauteng, North West and Free State provinces in South Africa, using the Nakamura *H/V* spectral ratio technique on records of the Orkney 5 August 2014 earthquake. The earthquake, of magnitude  $M_L = 5.5$ , led to the unfortunate death of one person and damage of more than 600 houses. Intensity data collected soon after the event showed that the effects of the earthquake appeared to vary significantly across the region. This motivated the authors to conduct a more detailed investigation of the effects of site conditions on seismic station records in the region. Resonance frequency values obtained from the *H/V* ratios were observed to vary strongly across the region and also within seismic station clusters. Similar behaviour was observed with the peak amplitude of the ratios at the resonance frequency, except for the Johannesburg area whose results showed a relatively simple shape of the ratios implying less complex velocity structure. All the *H/V* ratios exhibit dominant peaks at resonant frequencies that varied between 0.5 and 35 Hz. The average observed resonant frequency was  $f = 7.9$  Hz. The amplitude of the dominant peaks also varied strongly from 1.66 to 11.69, with only two sites exhibiting maximum peaks with amplitude smaller than 2. These results serve as a strong motivation or justification for the on-going microzonation studies in South Africa, where a detailed study of the velocity structure will be used to obtain reliable information on site amplification and resonance.

**Key words:** Site response, Orkney, Nakamura, South Africa, *H/V* ratios, resonance.

### 1. Introduction

It has been observed that earthquake ground motion and damage distribution are dependent on local geological conditions at the site (Zaharia et al. 2008; Bouranta et al. 2013; King and Tucker 1984; Aki 1988; Kawase 1996; Field and Jacob 1993; Nath et al. 2000, 2002a, b). The behaviour of the ground motion during an earthquake can be explained by the

geological surface structure, with the damage caused by strong earthquakes predominantly in sedimentary basins than on hard rock structures (Nakamura 2008). In the recent past, devastating damage was observed due to amplification of ground motion triggered as a consequence of local site conditions, such as during the famous Mexico City earthquake of 1985 (Singh et al. 1988), the Loma Prieta earthquake of 1989 (Hough et al. 1990), the Northridge earthquake of 1994 (Finn et al. 1995; Chang et al. 1996) and the Bhuj earthquake in India of 2001 (Hough et al. 2002). Site effects can be parameterized by factors such as resonance frequency, amplification factor, which have direct impact on resonance of certain building types, and thereby causing distortions or failures of constructions. The phenomenon through which seismic waves are trapped in sediments due to acoustic impedance contrast between sediments and the bedrock is what is defined as amplification of the ground motion (Zaharia et al. 2008). Recently, in South Africa, an earthquake of magnitude  $M_L 5.5$ , occurred on 5 August 2014 resulting in the death of one person and damage to more than 600 houses that were located close to the epicentre (Midzi et al. 2015). The earthquake was also felt as far as Gaborone in Botswana, Johannesburg, Pretoria and Durban with significant varying intensity levels, the highest being an MMI of VII close to the epicentral area (Fig. 1).

In some places, unexpectedly high-intensity values were observed and were suggested to be due to site amplification effects. Thus, it was decided to conduct further investigations to determine the possible effect of site conditions on the ground motion recorded by regional seismic stations during the earthquake. This decision was taken even knowing that some of the observed damage could probably be a contribution of poor construction practices. To reduce uncertainty on this question, site effects were

<sup>1</sup> Council for Geoscience, 280 Pretoria Street, Silverton, Pretoria, South Africa. E-mail: [vmidzi@geoscience.org.za](mailto:vmidzi@geoscience.org.za)

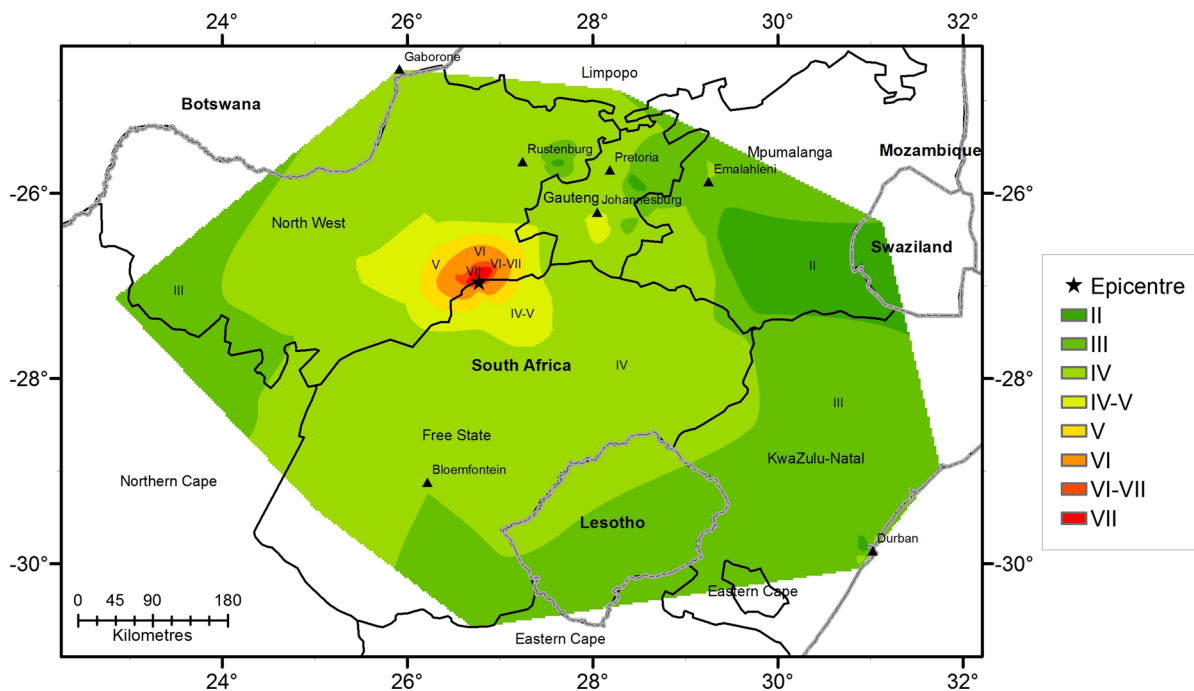


Figure 1  
The isoseismal map of the 5 August 2014 earthquake (Midzi et al. 2015)

investigated using the Earthquake Single Station Spectral Ratio (ESSSR) method (Nakamura 1989). This involved the calculation and analysis of horizontal to vertical ( $H/V$ ) spectral ratios using waveforms recorded at 37 different stations in the Gauteng, North West and Free State provinces of South Africa (Fig. 2).

## 2. Regional and Local Geological Setting

The geology of the study region was thoroughly discussed in two reports by Diop et al. (2015, 2016) prepared as part of the on-going microzonation study of Johannesburg and the Klerksdorp–Orkney–Stilfontein and Hartbeesfontein region (KOSH) in the North West province of South Africa. Presented here is a relevant summary of the geology of the Johannesburg region (Fig. 3) and KOSH area (Fig. 4).

The study area is underlain by important systems of rock from the basement units to quaternary deposits as shown in Figs. 3 and 4. The whole study area is largely underlain by the Kaapvaal Craton,

which formed between 3700 and 2700 Ma (Tankard et al. 1982; Hunter et al. 2006) and contains some of the oldest rocks on earth. As a result of its great age, its geology is diverse and complex, representing the result of numerous large-scale tectonic events, which created a large number of geological structures that can potentially be reactivated in future tectonic events. The Kaapvaal Craton consists predominantly of abundant granitoids that preserve metamorphosed remnants of volcano-sedimentary sequences and greenstone belts. The granitoids of the central Kaapvaal Craton include the Makoppa Dome and Gaborone Suite on the border with Botswana, the Kraaipan–Amalia area in central Northwest Province and the Vredefort and Johannesburg Domes closer to the central part of the study area (Robb et al. 2006). The basement below Johannesburg is formed by Archaean Granite with scattered greenstone remnants, forming the so-called Johannesburg Dome (Brandl et al. 2006). The Archaean Granite underlies the northern portion of the area and is unconformably overlain by the sediments of the Witwatersrand,

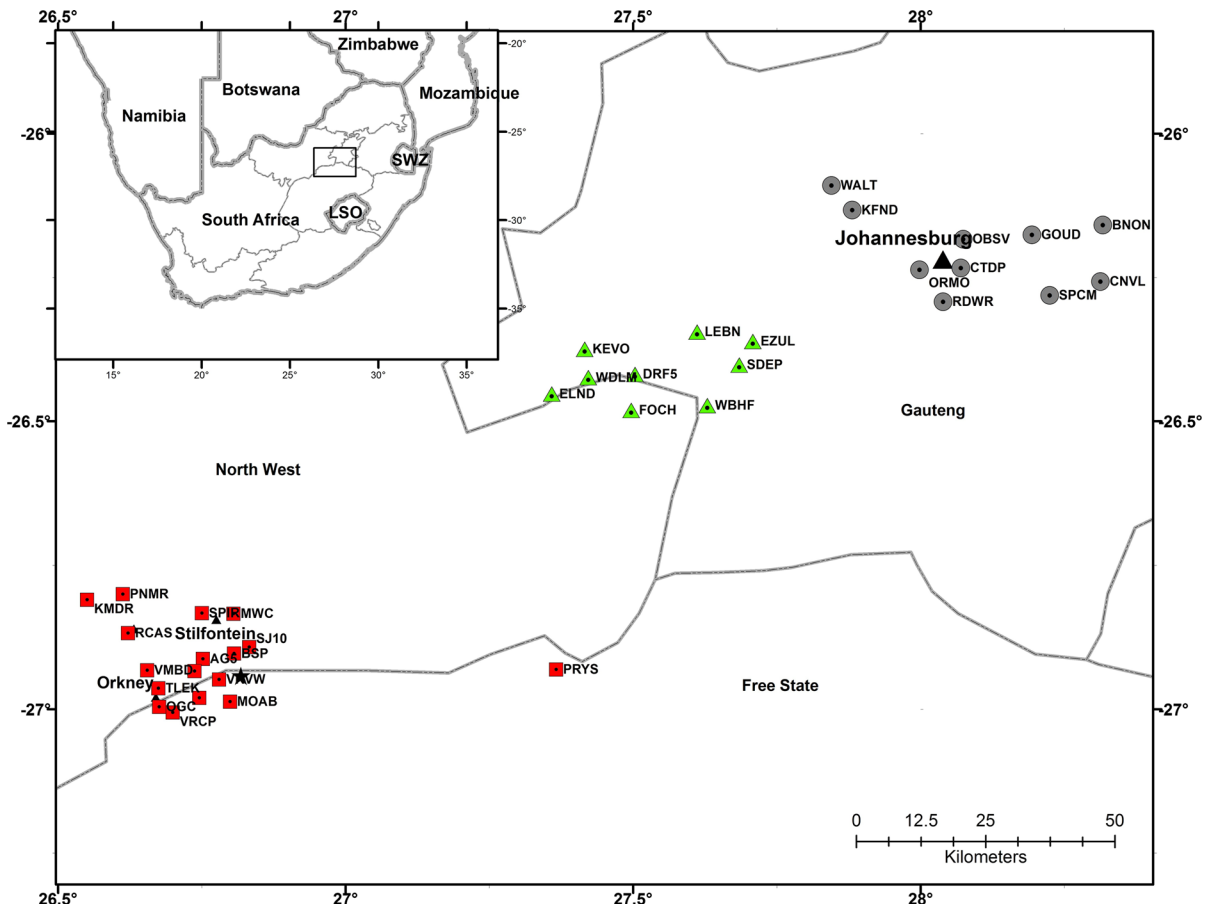


Figure 2

Thirty-seven seismic stations that recorded the magnitude  $M_L 5.5$ , 5 August 2014 earthquake and whose records were utilised in the site response analysis. Red squares with black dots in the centre represent KOSH stations; green triangles with black dots in the centre represent West Rand stations and grey circles with black dots in the centre present Johannesburg stations. The black star represents the epicentre of the Orkney earthquake. The study area is shown by the rectangle drawn in the map of southern Africa in the inset, where LSO stands for Lesotho and SWZ for Swaziland

Ventersdorp, and Transvaal Supergroups (Anhaeusser 2006; Diop et al. 2015).

The seismic stations in the Johannesburg and West Rand region are located on a variety of formations with some stations on the Malmani formation (KEVO, LEBN and SPCM), whilst other stations are found on the Klapperkop quartzite (ELND, DRF5 and SDEP), Timeball Hill (EZUL), Hospital Hill (KFND and OBSV), Turffontein (ORMO and CTD), Dwyka (BNOM and CNVL), Hekpoort (WDLM), Silverton (FOCH), Strubenkop (WBHF), Swazian (WALT), Kliprivierberg (RDWR) and Government (GOUD) (Fig. 3). The Timeball Hill Formation shale is overlain by the tholeiitic andesite of the Hekpoort

Formation, both belonging to the Pretoria group (Eriksson et al. 2006). The young Pretoria group units include the Daspoort quartzite Formation and the Silverton Formation shales intercalated with chert and volcanic agglomerate. The basal Hospital Hill Subgroup of the West Rand Group overlies the Dominion Group (Diop et al. 2015). Residual soils from quartzites of the Hospital Hill Subgroup are more resistant to weathering and consequently form outcropping. The residual quartzite is described in profile as moist, reddish brown blotched yellow, stiff, relict jointed and bedded, fine sandy silt with sub-angular to angular gravel of quartzite. In other instances, however, the Hospital Hill quartzite gives

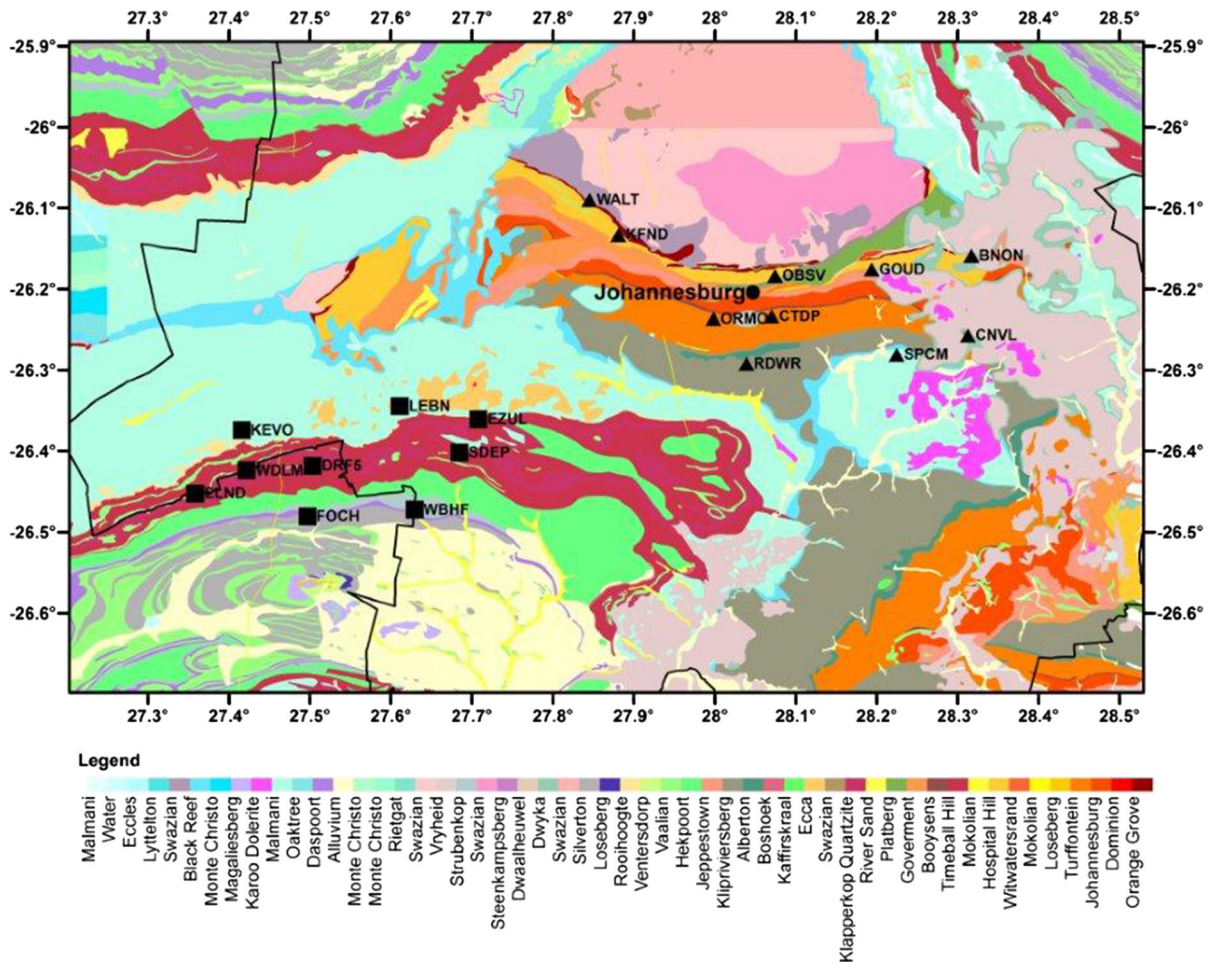


Figure 3

The geology of the Johannesburg and West Rand region. Also shown are locations of the seismic stations used in the site response analysis in the two regions, squares for stations in the West Rand and triangles for stations in the Central Rand (Johannesburg)

rise to deep residual yellow silty sands and sandy silts. Shales of the Hospital Hill Subgroup decompose to form pale red to dark reddish brown silty clays (Brink 1979). They are typically described as moist, reddish brown, stiff or very stiff, bedded and jointed sandy silt. The lower West Rand Group ( $3060 \pm 2$  Ma), predominantly argillaceous unit, and the upper Central Rand Group ( $2909 \pm 3$  Ma), predominantly arenaceous unit, are both composed of quartzites and shales, with the intercalated gold-bearing reef conglomerates.

In the area under discussion, the lower West Rand Group consists of 1500-m-thick alternating quartzite and shale of the Hospital Hill Subgroup (Diop et al.

2015). The Turffontein Subgroup overlays the Jeppesdorp Subgroup and contains an outlier of carboniferous shales and sandstones (Johnson et al. 2006). Residual soils from quartzites of the Turffontein subgroup usually occur as pinkish white and cream silty sand and exhibit relict jointed structure, directly underlining the hillwash and pedogenic soils. These residual quartzites extend down to depth of between 1 and 3 m below surface and are directly underlain by weathered quartzite bedrock. The average depth to bedrock is 2 m from existing ground level. Layers of Dwyka tillite occur below the Ecca Group lithologies in areas where percussion drilling was undertaken (Diop et al. 2015).

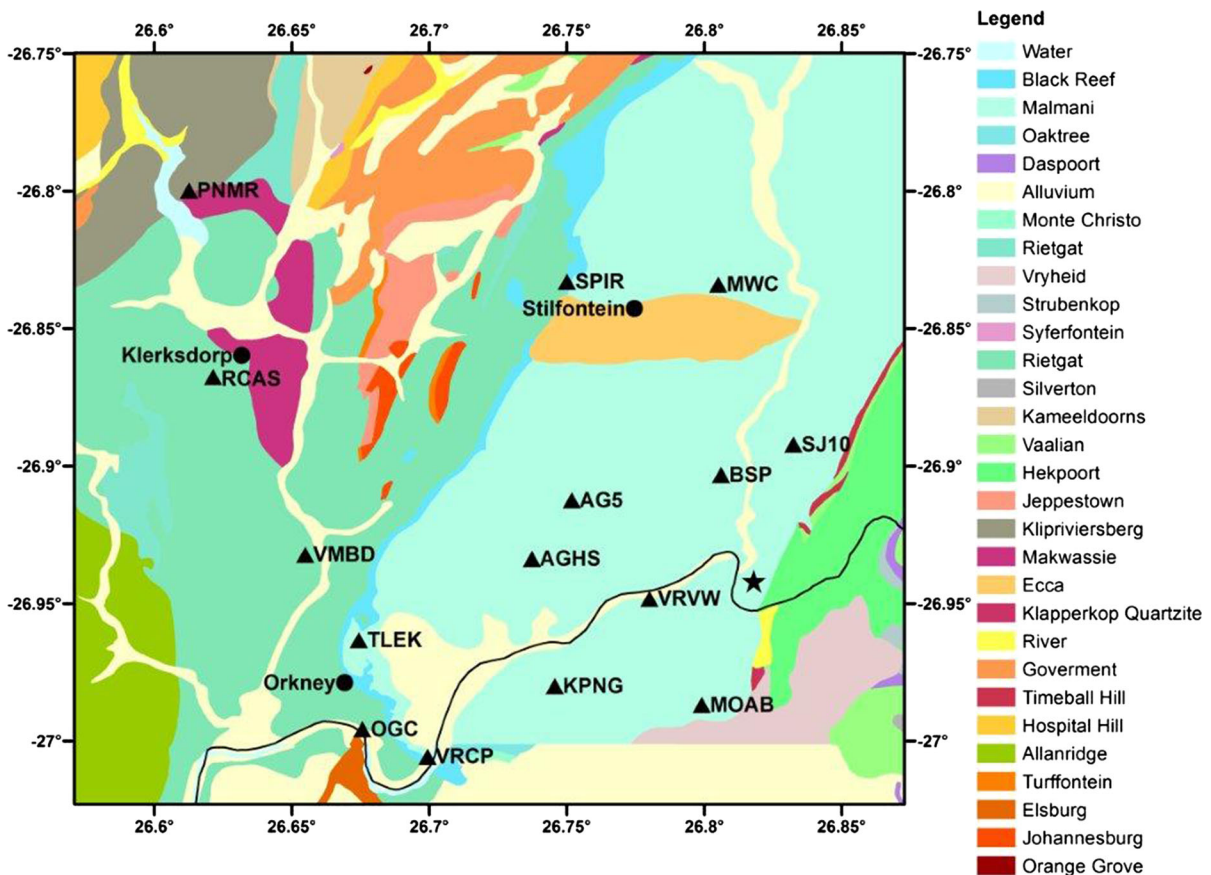


Figure 4

The geology of the KOSH region. Also shown are locations of the seismic stations that were used in the site response analysis in the region

The dominant formations on which most of the seismic stations are installed in the KOSH region are the Rietgat (RCAS and VMBD) and the Malmani (TLEK, KPNG, MOAB, VRVW, AGHS, BSP, AGS, SJ10 and MWC) (Fig. 4), whilst other stations are located on less-dominant formations including the Klipriviersberg (PNMR), Black Reef (SPiR) and on Alluvium deposits (OGC and VRCP). The Rietgat Formation covers a significantly large portion of the region, particularly, the central section from north to south, whilst the Malmani Subgroup of the Chuniespoort Group overlies the Black Reef Formation. According to Anhaeusser (2006), the Malmani Subgroup of the Transvaal Supergroup is subdivided into five formations by the following criteria: chert content, stromatolite morphology, intercalated shales and the erosion surfaces. These formations are (from

oldest to youngest): Oaktree, Monte Cristo, Lyttelton, Eccles and the Frisco Formations and are composed of dolomite and limestone as carbonaceous rocks intercalated with subordinate chert and carbonaceous shale, mudstones as well as quartzite. The Malmani Subgroup covers a large part of the eastern section of the region.

A significant portion of the KOSH region is also covered by miscellaneous fills described as thick, poorly compacted and highly variable soils, which are overlain by very weak and highly compressible alluvial and/or colluvial soils (Diop et al. 2016). Though the fills are said to be variable in nature and composition, they commonly comprise loose to dense or stiff intact slightly clayey silty sand with scattered gravels and boulders as well as ash layers, bricks, cinder, rock rubble, soils, refuse and occasionally

builder's rubble and mine sand. The thickness of the fill layers varies widely from 0 m to more than 3.5 m and could be up to 5.0 m deep in some places. Due to its nature, it is observed to collapse easily on excavation. Consequently, it is highly unlikely that structures could be built on them (Diop et al. 2016).

Transported soils also play a major role in the geology of the region. These include Aeolian sand deposits, hillwash, colluvium and alluvial deposits. Aeolian sands are generally reddish brown, silty sand with trace amounts of sub-rounded gravels of mixed origin. According to Diop et al. (2016), the average thickness of their layers varies widely from 0 m to more than 5 m, and could locally reach up to 8 m in some places. They are mapped mainly in areas south of Orkney. Alluvial deposits are the results of river and drainage channel processes through the area. They are homogenous dark, soft to firm clay layers of variable thicknesses especially near the Vaal River and cover the general bank area of the River (Diop et al. 2016). Two seismic stations, VRCP and OGC, appear to be located in such areas (Fig. 4), while station VRVW though located on the Malmani formation is not too far from the banks of the river. However, colluvium soils are the most common uppermost layer of the soil horizons in the area. These are mainly dark brown to reddish, loose to medium dense, silty sand or clayey silty sand layers of variable thickness.

### 3. Single Station Spectral Ratio (SSSR) Method

One of the most widely used methods for site response estimation is the so-called Nakamura's technique (Nakamura 1989). In many studies (e.g., Ohmachi et al. 1991; Field and Jacob 1993; Lachet et al. 1996; Fah et al. 1997), this technique has been shown to be stable, reliable and gives a clear peak correlated with the resonant frequency especially on soft soil. However, there is still doubt on its effectiveness to determine the amplification factor, though the results give a reliable indication of relative amplification (e.g., Lermo and Chávez-García 1994; Bard 1999; Horike et al. 2001; Bonnefoy-Claudet et al. 2008). This technique, initially introduced by Nogoshi and Igarashi (1971), consists in taking the

ratio between the Fourier spectra of the horizontal and vertical components of the ambient vibrations. It is inexpensive, can be applied to regions of low seismicity and only requires data from a single station (Bouranta et al. 2013). Contrary to the traditional method of applying this technique to ambient noise records, the technique was applied in this study to strong motion records recorded during the 5 August 2014, magnitude  $M_L 5.5$  Orkney earthquake.

The phenomenon responsible for the amplification of the ground motion in areas with soft sediments is the trapping of seismic waves within sediments due to the acoustic impedance contrast (the product between the mean velocity of the seismic wave in a layer and its mean density) between sediments and bedrock (Zaharia et al. 2008). The interference of these "trapped" waves leads to resonances whose shapes and frequencies are well correlated with the geometrical and mechanical characteristics of the structure (Nakamura 2008).

### 4. Data Used

The *H/V* spectral ratios in this study were computed using S wave windows of the 5 August 2014 magnitude  $M_L 5.5$  earthquake recorded on 37 seismic stations (Fig. 2) operated by the Council for Geoscience. The S wave windows were of varying lengths depending on the epicentral distance of the recording stations. Of the 37 stations, two (KMDR and WDLM) are equipped with 3T Guralp full broadband sensors, another two (PRYS and SWZ) with 40T Guralp semi-broadband sensors, whilst the rest of the stations (33) are equipped with Kinematics, EpiSensor force balance accelerometers. The data were processed using the Geopsy software package. On average, ten windows of about 2 s were automatically selected using an anti-STA/LTA trigger algorithm. A cosine window tapering of 5% and a Konno-Ohmachi smoothing with a bandwidth of 20 were applied. The Fourier spectra of the three components were calculated, and then the average of the horizontal components was taken and divided by the vertical component to calculate the *H/V* spectral ratio. The waveforms shown in Fig. 5 are an example of the S wave window selected for TLEK station,

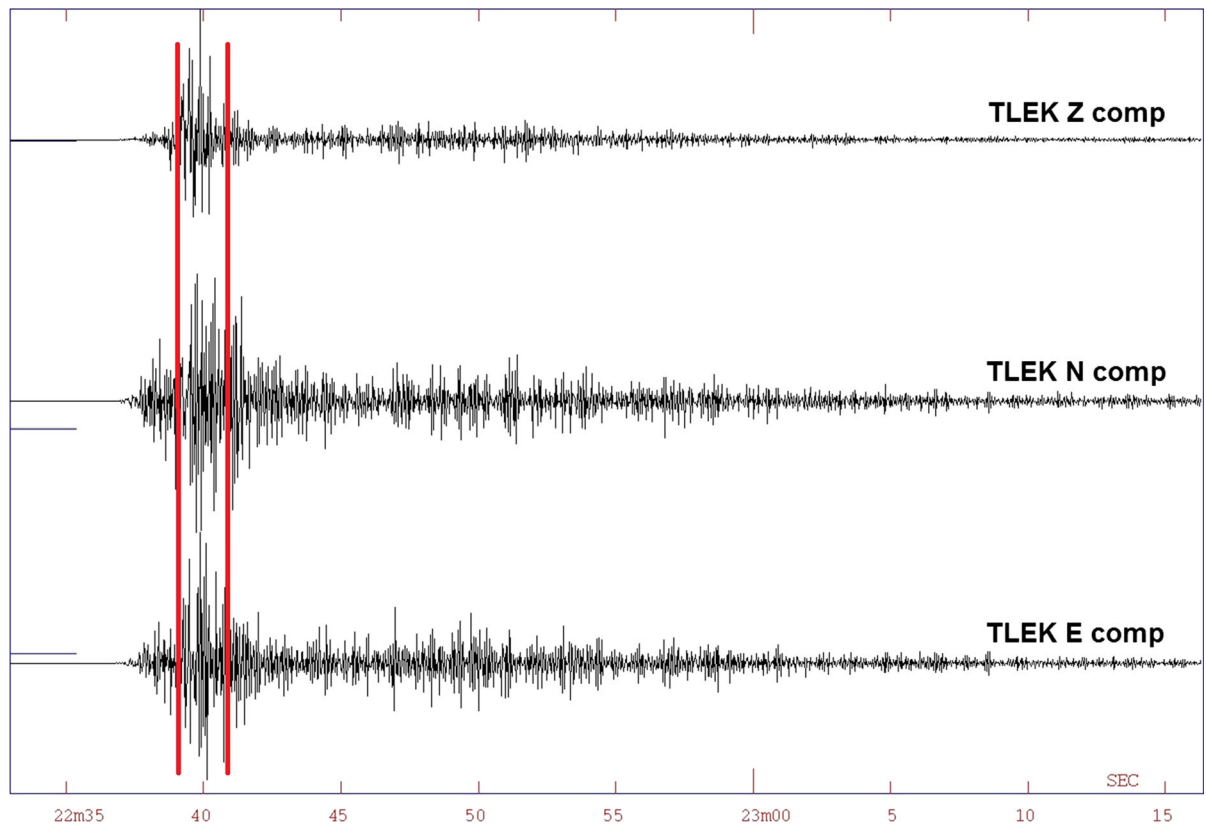


Figure 5

The three-component (vertical, Z and two horizontal, N and E) ground accelerations recorded at the station TLEK generated by the 5 August 2014 Orkney earthquake. The red lines indicate the direct S wave window that was used in the computation of the  $H/V$  spectral ratio for TLEK station

which is one of the stations equipped with the Kinometrics EpiSensor.

### 5. Results and Discussion

Following the procedure described above in Sects. 3 and 4, 37  $H/V$  spectral ratios were calculated. The ratios were calculated for frequency ranging from 0 to 50 Hz. The results, presented in Fig. 5 and Table 1, show that all the spectral  $H/V$  ratios exhibit dominant peaks which vary between 0.5 and 35 Hz. The average frequency of the maxima of these peaks is  $f = 7.9$  Hz. The amplitude of these peaks varies strongly from 1.66 at WDLM to a high of 11.69 at BSP (Fig. 6, Table 1), with only two sites (WALT and WDLM) exhibiting peaks with amplitude smaller

than 2. The strong difference in peak amplitudes and their shapes, as well as the multiple peaks observed (e.g., strong at AGHS, BNON, BSP, CTD, EZUL, KFND, KMDR, MWC, OBSV, SPIR and WDLM) suggests significant lateral variations and impedance contrasts within the subsoil of the region. On comparing the shape of the  $H/V$  spectral ratios across the region (Fig. 6), no particular trend is clearly observed, but rather strong differences. Similarly, differences of the ratios are also seen within the KOSH (Fig. 6a) and West Rand (Fig. 6b) clusters. On the other hand, the shapes of ratios in the Johannesburg (Fig. 6c) cluster are generally similar in their simple structure especially after the sharp first impulse. This implies that the shallow structure in that region is not complex per site as well as spatially.

Table 1

*The fundamental frequency and H/V spectral ratio amplitudes observed at the 37 stations that recorded the 5 August 2014 earthquake*

ID	Station	Longitude	Latitude	Fundamental frequency (Hz)	H/V ratios
0	AG5	26.7517	− 26.9125	8.94325	8.84
1	AGHS	26.7372	− 26.9338	2.92851	2.86
2	BNON	28.317	− 26.159	6.08951	2.85
3	BSP	26.806	− 26.9033	2.01851	11.69
4	CNVL	28.3127	− 26.2572	8.53676	2.22
5	CTDP	28.0701	− 26.2336	11.2851	2.6
6	DRF5	27.5034	− 26.4183	12.3854	3.25
7	ELND	27.3583	− 26.4525	3.06795	5.29
8	EZUL	27.7082	− 26.3609	1.83919	3.92
9	FOCH	27.4968	− 26.4809	2.66835	2.01
10	GOUD	28.1936	− 26.1759	6.16423	3.45
11	KEVO	27.4156	− 26.3744	6.44427	3.53
12	KFND	27.881	− 26.133	4.88505	2.91
13	KMDR	26.5504	− 26.8096	2.66835	4.34
14	KPNG	26.7455	− 26.9801	16.0727	3.14
15	LEBN	27.6111	− 26.3447	2.11462	6.55
16	MOAB	26.799	− 26.9869	3.21404	4.98
17	MWC	26.805	− 26.834	1.83919	5.61
18	OBSV	28.0742	− 26.1835	10.7722	2.34
19	OGC	26.6756	− 26.9958	2.4313	4.63
20	ORMO	27.9982	− 26.2368	8.94325	3.13
21	PNMR	26.6125	− 26.7999	31.4015	3.21
22	PRYS	27.366	− 26.931	0.899873	8.75
23	RCAS	26.6213	− 26.8676	10.1826	8.07
24	RDWR	28.0391	− 26.2922	26.0841	4.86
25	SDEP	27.6846	− 26.402	3.87132	2.93
26	SJ10	26.8323	− 26.8922	5.91631	8.45
27	SPCM	28.2246	− 26.281	3.5274	4.18
28	SPIR	26.75	− 26.833	3.06795	3.76
29	SWZ	25.332	− 27.182	0.51147	7.98
30	TLEK	26.6743	− 26.9634	9.8152	2.88
31	VMBD	26.6548	− 26.9323	8.94325	4.01
32	VRCP	26.6993	− 27.0057	5.00135	8.59
33	VRVW	26.78	− 26.9483	4.05565	10.14
34	WALT	27.845	− 26.09	11.2851	1.89
35	WBHF	27.6291	− 26.4725	5.36134	4.18
36	WDLM	27.422	− 26.424	35.4119	1.66

On comparing the *H/V* response results to preliminary microzonation results for Johannesburg and KOSH (Rathod et al. 2018a, b; Birch et al. 2017), *H/V* amplitude ratios in the Johannesburg area are seen to vary according to  $V_{s30}$  and depth to bedrock values, with low ratios observed in areas of high  $V_{s30}$  (Fig. 7a) and deeper depth to bedrock (Fig. 7b). Such a trend is not as clearly visible in the KOSH area, where high amplitude ratios are observed in areas of high  $V_{s30}$  (i.e., areas with shallow bedrock as in Fig. 7c). However, it should be noted that this can

occur in areas with high bedrock—soil impedance contrast. Unfortunately, the microzonation data available does not allow the determination of these values in that particular part of the region.

The distribution of the resonance frequency (Fig. 8) does not show a strong trend in the values across the region, though some variation is seen between the KOSH cluster and the Johannesburg cluster where the frequency values on average appear to increase. Similarly, strong variations are observed within each cluster of *H/V* ratios. On the other hand,



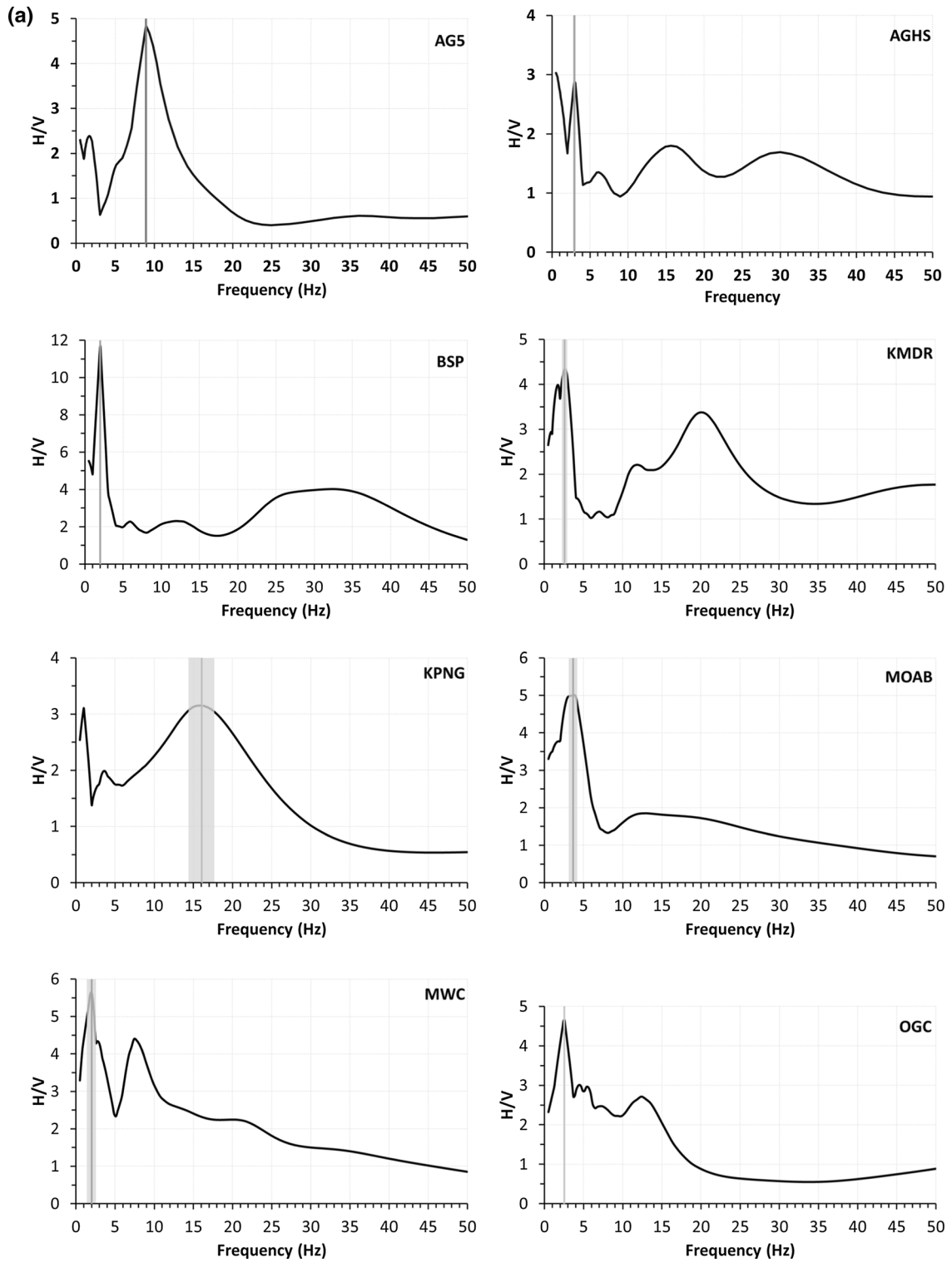


Figure 6

**a** Plots showing  $H/V$  ratios obtained for KOSH seismic stations. **b** Plots showing  $H/V$  ratios obtained for West Rand seismic stations. **c** Plots showing  $H/V$  ratios obtained for Johannesburg seismic stations

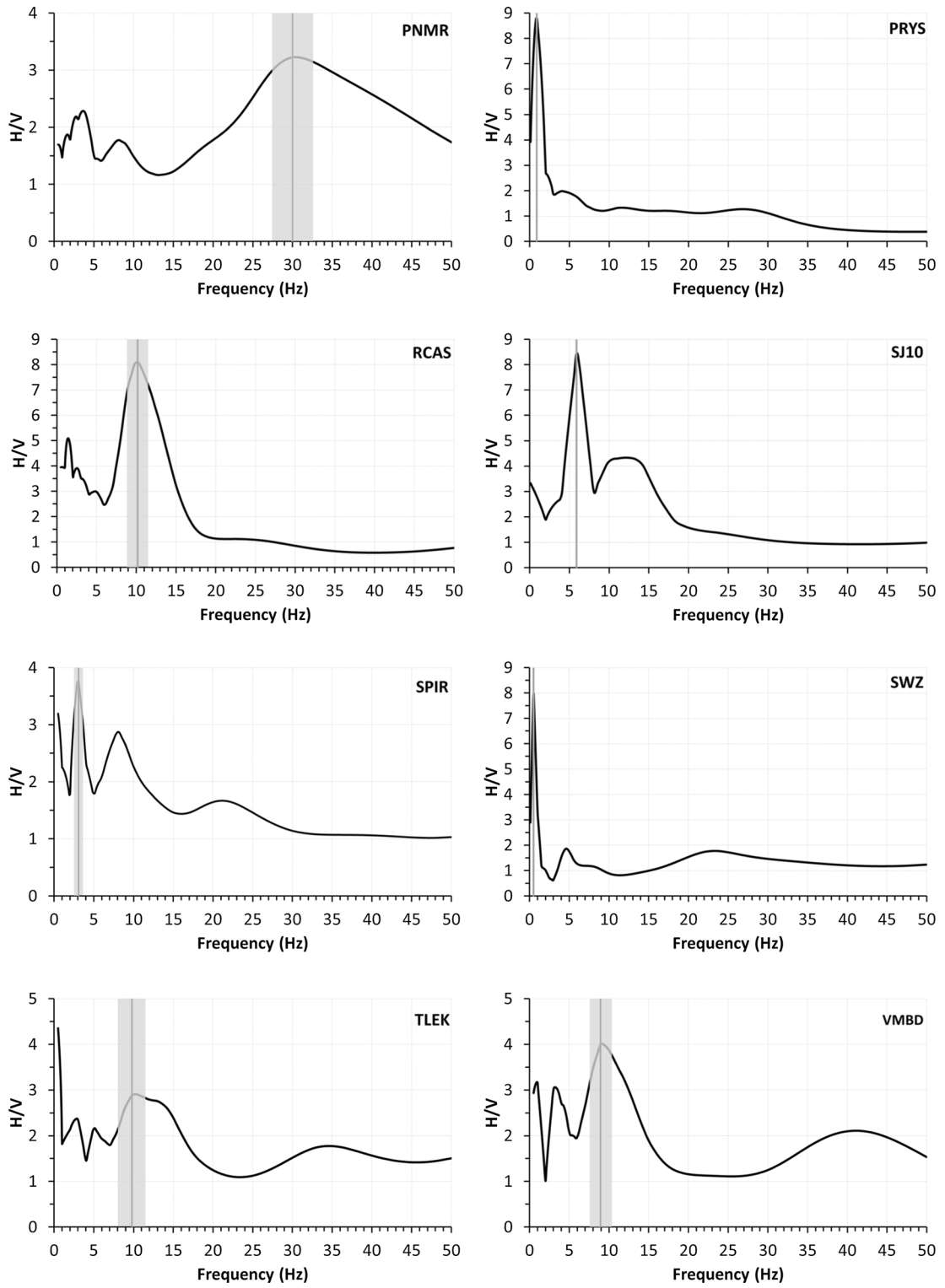


Figure 6 continued

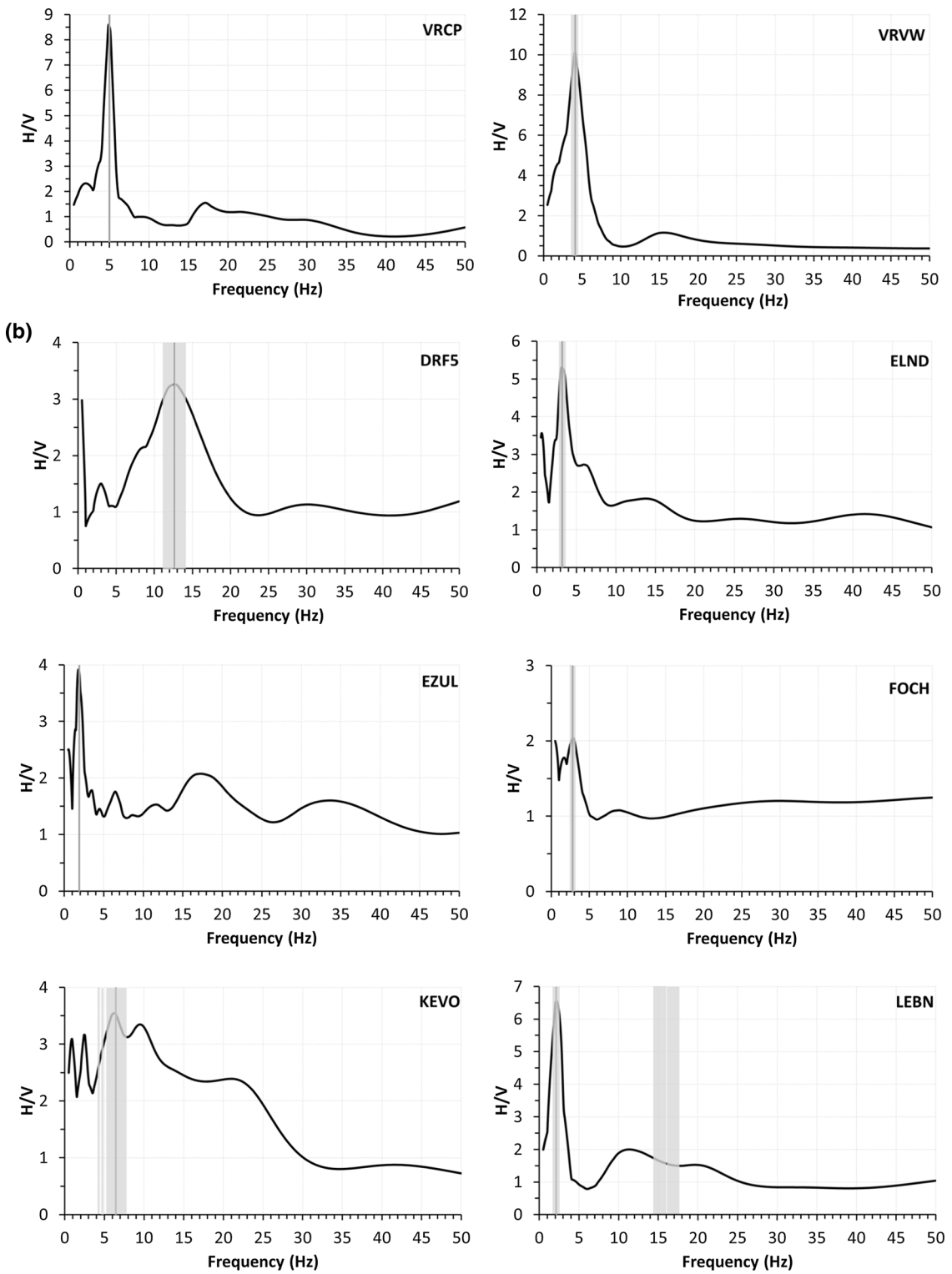


Figure 6 continued

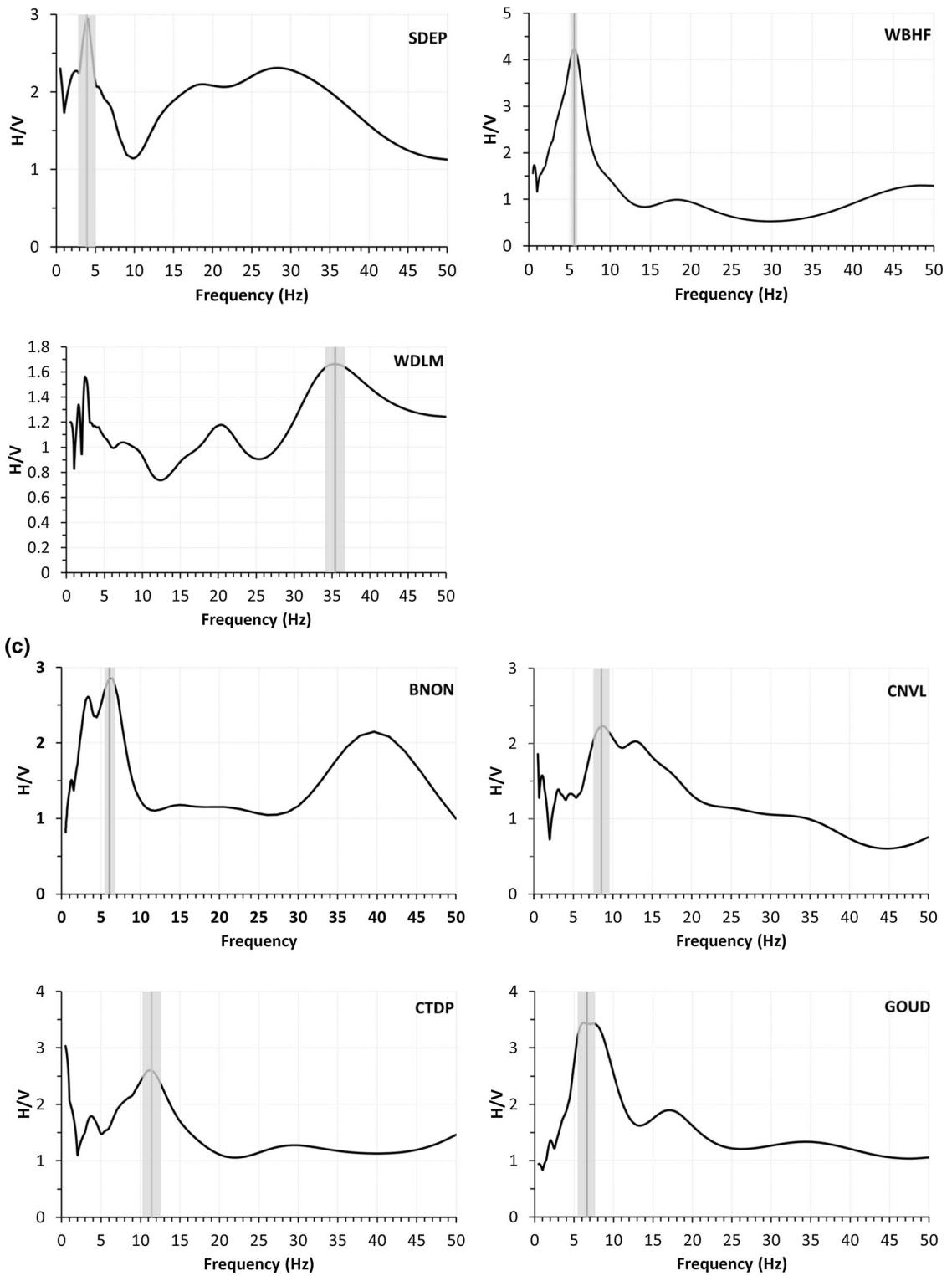
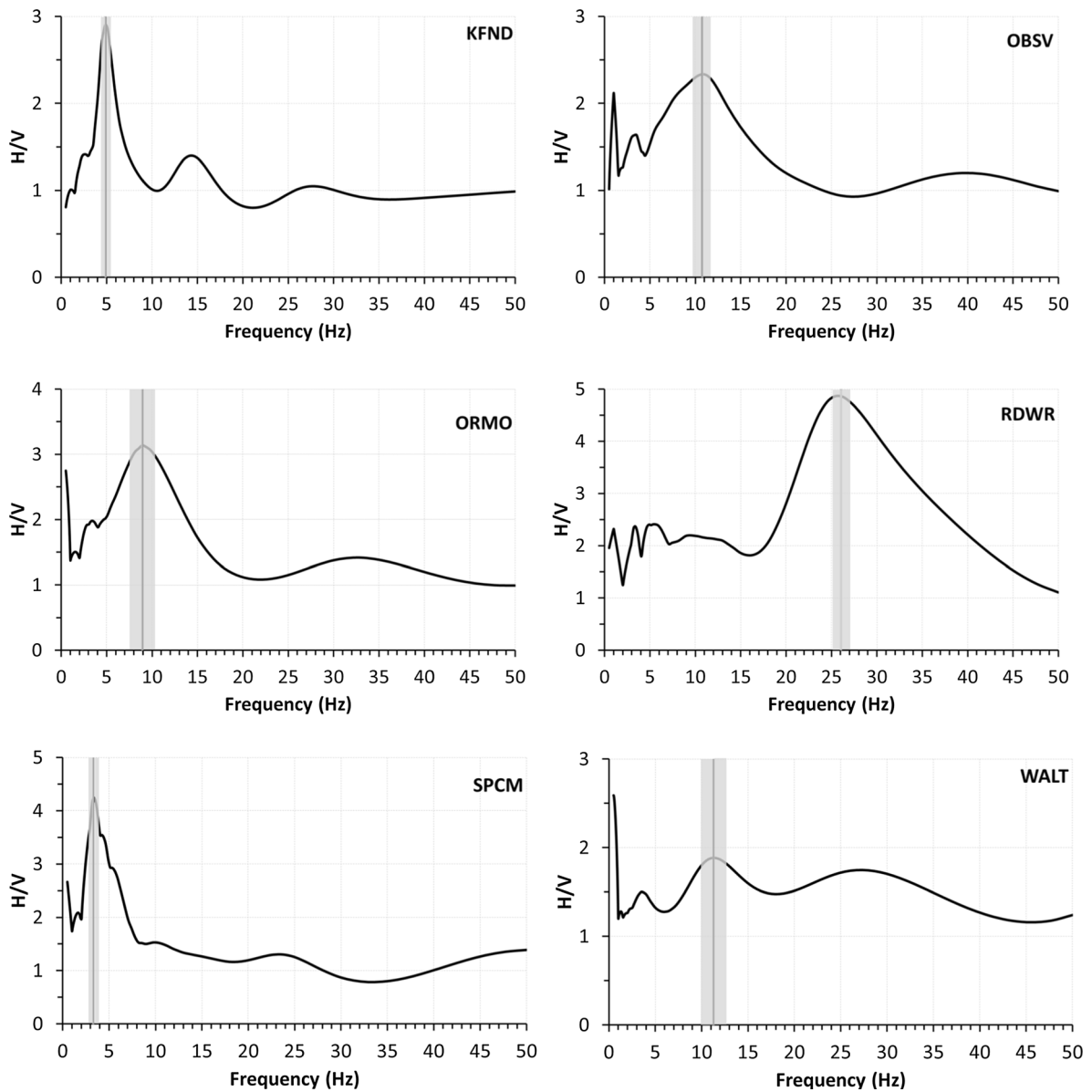


Figure 6 continued

Figure 6  
continued

a clear trend is observed showing a decrease in H/V ratio amplitude from KOSH to Johannesburg (Fig. 9). This variation in amplitude reinforces the conclusion that there is a significant variation in subsurface structure in the region, which appears to become simpler in the Johannesburg sub-region. The lower ratio amplitudes in this Johannesburg region also imply a weaker impedance contrast between the bedrock and upper surface structure.

Fundamental frequencies of the sites in the Johannesburg municipality and KOSH area were also compared to depth to bedrock as in the preliminary microzonation study results (Rathod et al. 2018a, b; Birch et al. 2017). In Johannesburg, no clear trend can be observed (Fig. 10a), though some of the higher frequency sites appear to coincide with areas of shallow depth to bedrock as expected. Those sites on deeper depth to bedrock have lower frequencies of

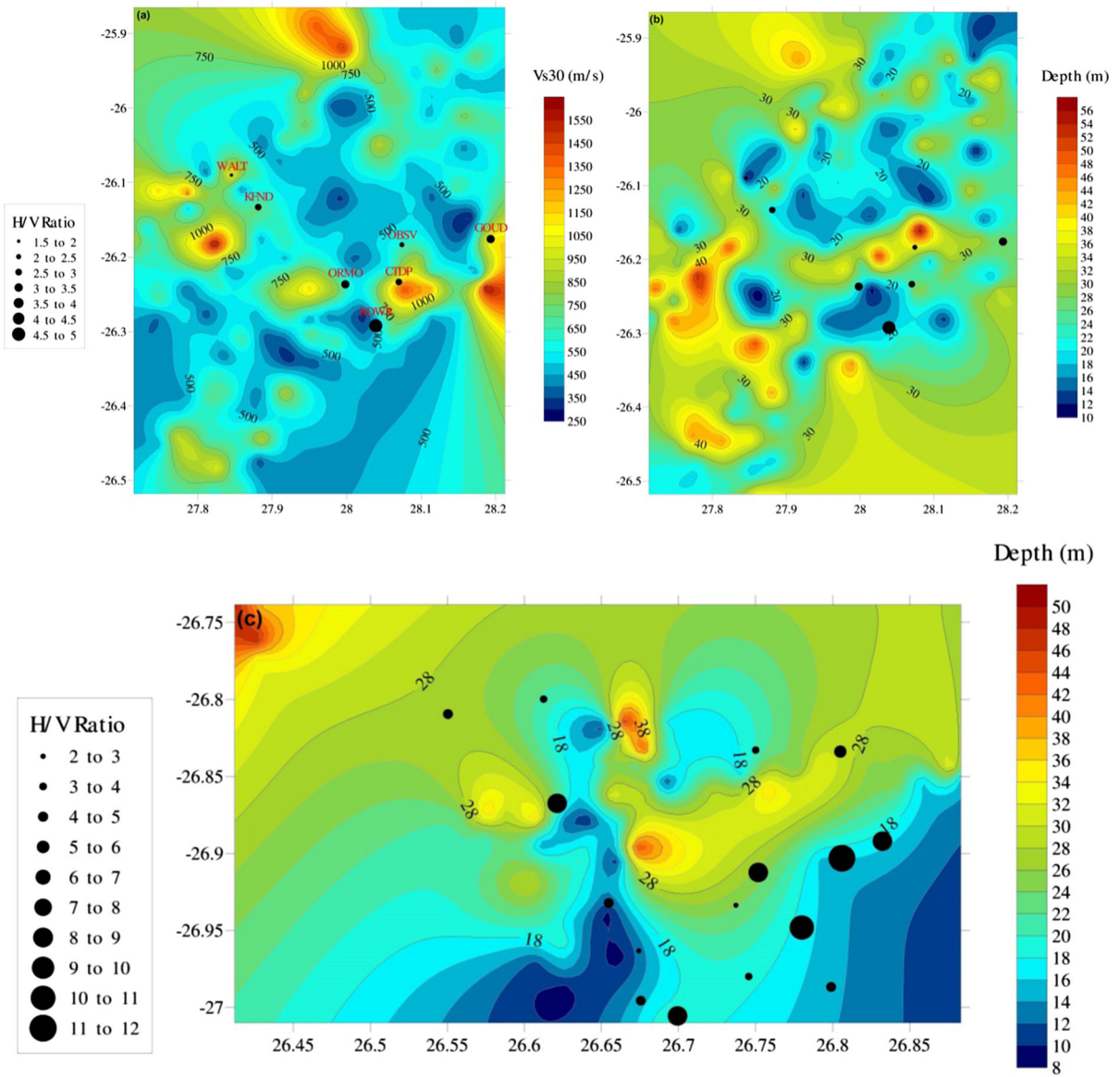


Figure 7

Comparison of H/V ratio amplitude to **a**  $V_{s30}$  spatial variation in Johannesburg, **b** depth to bedrock also in Johannesburg and **c** depth to bedrock in the KOSH area

less than 10 Hz. Similarly, no clear trend was observed in the KOSH area (Fig. 10b).

6. Conclusion

The *H/V* ambient vibration method (Nakamura's technique) has become one of the most popular

methods for estimating site response in urban areas. In this study, the same technique was applied, but on an S wave window of a moderately sized earthquake ( $M_L 5.5$ ) that occurred in the KOSH region on 5 August 2014 and was well recorded by 37 seismic stations. The computed *H/V* spectral ratios exhibit dominant peaks varying between 0.5 and 35 Hz across the whole study region. The average frequency

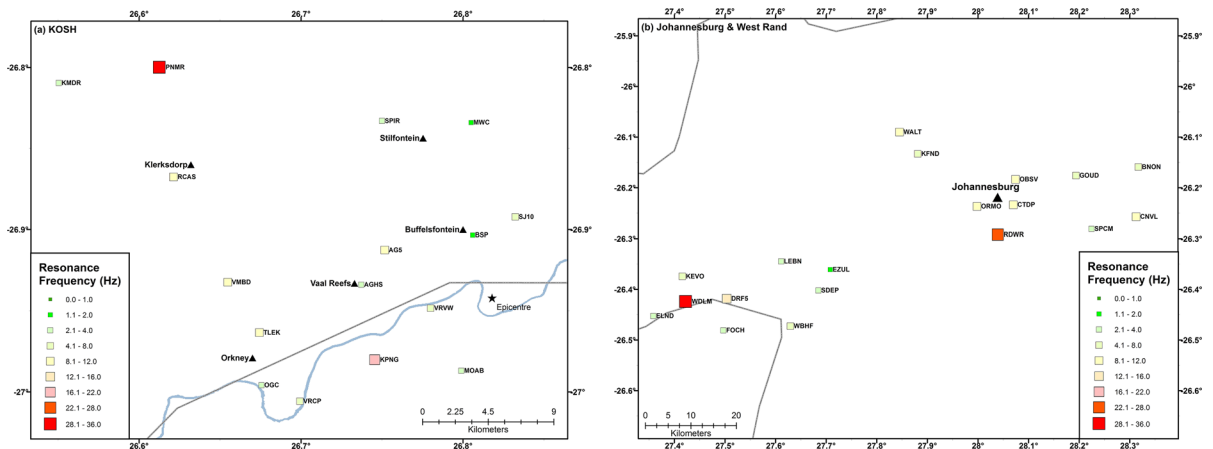


Figure 8

Spatial distribution of resonant fundamental frequencies obtained from  $H/V$  ratios calculated at the 37 stations in the KOSH region (a) and in the Johannesburg and West Rand region (b). Size of symbols is proportional to measured value

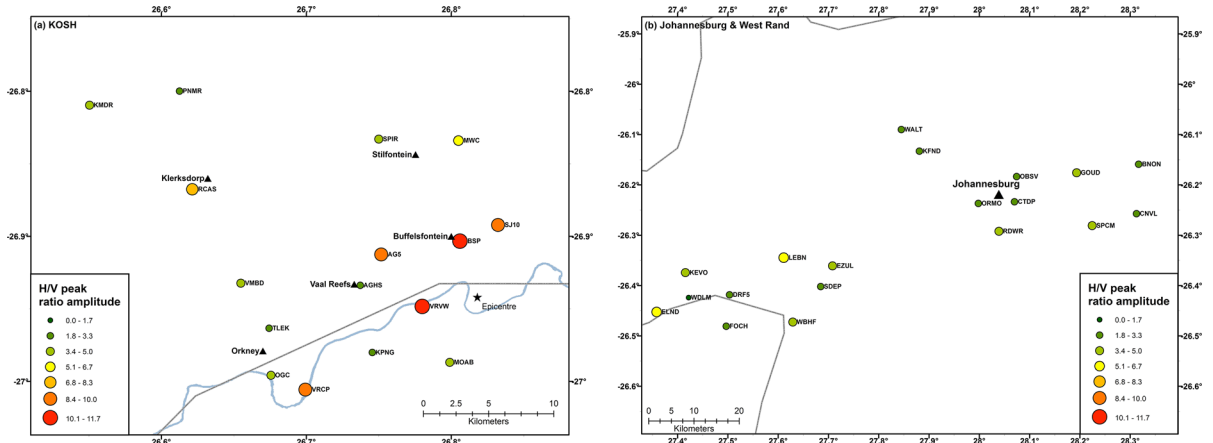


Figure 9

Variation in  $H/V$  resonant peak ratio amplitudes calculated for the 37 stations in the KOSH region (a) and in the Johannesburg and West Rand region (b). Size of symbols is proportional to measured value

of the maxima of these peaks is  $f = 7.9$  Hz. Apart from a strong spatial variation across the region, a significant variation was also observed within the three clusters of spectral ratios. The variation was also observed in the peak amplitudes of the  $H/V$  spectral ratios across the same region, but with those in the Johannesburg area showing smaller deviations. The complex shapes of the ratios observed imply complex or heterogeneous structure in the region except for the Johannesburg region whose results appear to be simpler.

The results from this study strongly suggest a complex response at sites in the region to earthquake ground motion. The  $H/V$  amplitude ratios in the Johannesburg area are low in areas of high  $V_{s30}$  and deeper depth to bedrock. Unfortunately, such a trend is not as clearly visible in the KOSH area, where high amplitude ratios are observed in areas of high  $V_{s30}$  and shallow bedrock, though such behaviour can occur in areas with high bedrock—soil impedance contrast. Unfortunately, the data available does not allow the determination of these values in that particular part of the region.

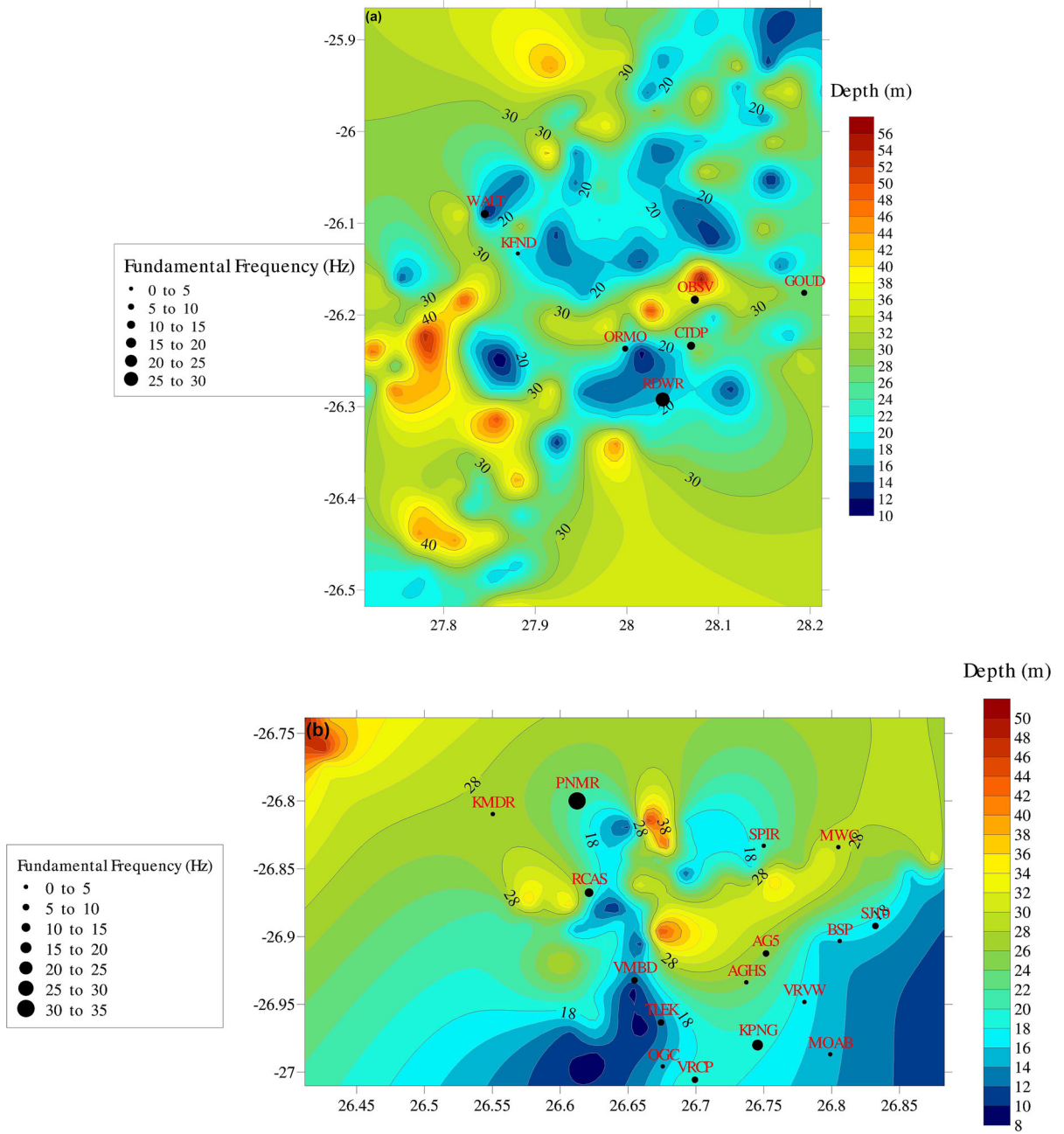


Figure 10 Comparison of fundamental frequency values to depth to bedrock in (a) Johannesburg and (b) KOSH area

*Acknowledgements*

The authors are grateful to the Council for Geoscience for allowing them to make use of the data

recorded by the national and cluster networks for the analysis as well as permission to spend time on this work.



## REFERENCES

- Aki, K. (1988). Local site effects on ground motion. Earthquake engineering and soil dynamics ii-recent advances in ground motion evaluation. Proc. of the A.S.C.E. Speciality Conference, Park City, Utah, June 27–30, pp. 103–155.
- Anhaeusser, C. R. (2006). Ultramafic and Mafic intrusions of the Kaapvaal Craton. In M. R. Johnson, C. R. Anhaeusser, & R. J. Thomas (Eds.), *The geology of South Africa* (pp. 95–134). Pretoria: Geological Society of South Africa, Johannesburg/Council for Geoscience, South Africa.
- Bard, P.Y. (1999). Micro tremor measurements: a tool for site effect estimation? Proceedings of the 2nd International Symposium on the Effect of Surface Geology on Seismic Motion, Yokohama, Japan, pp. 1251–1279.
- Birch, D.J., Mulabisana, T., Manzunzu, B., Pule, T., Zulu, B. & Myendekei, S. (2017). Investigating 1-D shear-wave velocity profiles using the MASW method in Johannesburg and KOSH. Council for Geoscience report number, 2017-0053.
- Bonnefoy-Claudet, S., Köhler, A., Cornou, C., Wathelet, M., & Bard, P. Y. (2008). Effects of love waves on microtremor H/V ratio. *Bulletin of the Seismological Society of America*, 98(1), 288–300.
- Bouranta, E., Vallianatos, F., Hatzopoulos, J. N., Papadopoulos, I., & Gaganis, P. (2013). Microtremor HVSR study of site effects in the urban area of the Town of Mytilene, Lesvos (Greece)—preliminary results. *Bulletin of the Geological Society of Greece*, XLVII, 1081–1089.
- Brandl, G., Cloete, M., & Anhaeusser, C. R. (2006). Archaean greenstone belts. In M. R. Johnson, C. R. Anhaeusser, & R. J. Thomas (Eds.), *The geology of South Africa* (pp. 9–56). Pretoria: Geological Society of South Africa, Johannesburg/Council for Geoscience, South Africa.
- Brink, A. B. A. (1979). *Engineering geology of Southern Africa* (Vol. 1). Pretoria: Building Publications.
- Chang, S. W., Bray, J. D., & Seed, R. B. (1996). Engineering implications of ground motions from the Northridge earthquake. *Bulletin of the Seismological Society of America*, 86(1B), S270–S288.
- Diop, S., Heath, L., Kekana, E., Mahandana, N., Mkhize, N., Motjale, P., Msane, B., Msomi, P., Mutshekwa, N., Ngoato, T., Nkosi, S., Nxumalo, N., Seanego, P., Sebeyi, T., Sebesho, M. & Zungu, N. (2015). Subsurface geotechnical evaluation of the city of Johannesburg in microzonation of Johannesburg. Council for Geoscience, Report number, 2015-0066.
- Diop, S, Heath, L., Malepe, M., Motjale, P., Mpanza, N., Msane, B., Radzilani, M., Rikhotso, J., Sebesho, M., Skhosana, B. & Zungu, N. (2016). Geotechnical assessment of the KOSH area for seismic microzonation. Council for Geoscience, Report number, 2016-0079.
- Eriksson, P. G., Altermann, W., & Hartzler, F. J. (2006). The transvaal supergroup and its precursors. In M. R. Johnson, C. R. Anhaeusser, & R. J. Thomas (Eds.), *The Geology of South Africa* (pp. 237–260). Pretoria: Geological Society of South Africa, Johannesburg/Council for Geoscience, South Africa.
- Fah, D., Ruttener, E., Noack, T., & Kruspan, P. (1997). Microzonation of the city of Basel. *Journal of Seismology*, 1, 87–102.
- Field, E. H., & Jacob, K. (1993). The theoretical response of sedimentary layers to ambient seismic noise. *Geophysical Research Letters*, 20(24), 2925–2928.
- Finn, W. D. L., Ventura, C. E., & Schuster, N. D. (1995). Ground motions during the 1994 Northridge earthquake. *Canadian Journal of Civil Engineering*, 22, 200–315.
- Horike, M., Zhao, B., & Kawase, H. (2001). Comparison of site response characteristics inferred from microtremors and earthquake shear wave. *Bulletin of the Seismological Society of America*, 91, 1526–1536.
- Hough, S. E., Borchardt, R. D., Friberg, P. A., Busby, R., Field, E. H., & Jacob, K. E. (1990). The role of sediment induced amplification in the collapse of the Nimitz freeway during October 17, 1989 Loma Prieta earthquake. *Nature*, 344, 853–855.
- Hough, S. E., Martin, S., Bilham, R., & Atkinson, G. M. (2002). The 26 January 2001 M 7.6 Bhuj, India, Earthquake: observed and predicted ground motions. *Bulletin of the Seismological Society of America*, 92(6), 2016–20179.
- Hunter, D. R., Johnson, M. R., Anhaeusser, C. R., & Thomas, R. J. (2006). Introduction. In M. R. Johnson, C. R. Anhaeusser, & R. J. Thomas (Eds.), *The geology of South Africa* (pp. 1–7). Pretoria: Geological Society of South Africa/Council for Geoscience, South Africa.
- Johnson, M. R., Van Vuuren, C. J., Visser, J. N. J., Cole, D. I., de Wickens, D., Christie, A. D. M., et al. (2006). Sedimentary rocks of the Karoo Supergroup. In M. R. Johnson, C. R. Anhaeusser, & R. J. Thomas (Eds.), *The Geology of South Africa* (pp. 461–500). Pretoria: Geological Society of South Africa/Council for Geoscience, South Africa.
- Kawase, H. (1996). The cause of the damage belt in Kobe: the basin-edge effect, constructive interference of the direct S-wave with the basin induced diffracted/Rayleigh waves. *Seismological Research Letters*, 67(5), 25–34.
- King, J. L., & Tucker, B. E. (1984). Observed variations of earthquake motion across a sediment-filled valley. *Bulletin of Seismological Society of America*, 74, 153–165.
- Lachet, C., Hazfield, D., Bard, P. Y., Theodulidis, N., Papaioannou, C., & Savvaids, A. (1996). Site effects and microzonation in the city of Thessaloniki (Greece) comparison of different approaches. *Bulletin of the Seismological Society of America*, 86, 1692–1703.
- Lermo, J., & Chávez-García, F. J. (1994). Are microtremors useful in site response evaluation? *Bulletin of the Seismological Society of America*, 84, 1350–1364.
- Midzi, V., Zulu, B. S., Manzunzu, B., Mulabisana, T., Pule, T., Myendekei, S., et al. (2015). Macroseismic survey of the ML5.5, 2014 Orkney earthquake. *Journal of Seismology*, 19, 741–751.
- Nakamura, Y. (1989). A method for dynamic characteristics estimation of subsurface using microtremor on the ground surface. *RTRI Quarterly Report Number*, 30(1), 25–33.
- Nakamura, Y. (2008). On the H/V spectrum. The 14th World Conference on Earthquake Engineering, Beijing, China.
- Nath, S. K., Biswas, N. N., Dravinski, M., & Papageorgiou, A. (2002a). Determination of S-wave site response in anchor-age, Alaska in the 1–9 Hz frequency band. *Pure and Applied Geophysics*, 159, 2673–2698.
- Nath, S. K., Sengupta, P., & Kayal, J. R. (2002b). Determination of site response at Garhwal Himalaya from the aftershock sequence of 1999 Chamoli earthquake. *Bulletin of the Seismological Society of America*, 92, 1071–1081.
- Nath, S. K., Sengupta, P., Sengupta, S., & Chakrabarti, A. (2000). Site response estimation using strong motion network: A step towards microzonation of Sikkim Himalayas. *Current Science: Special Session, Seismology*, 2000(79), 1316–1326.

- Nogoshi, M., & Igarashi, T. (1971). On the amplitude characteristics of microtremor – Part 2. *Journal of the Seismological Society of Japan*, 24, 26–40.
- Ohmachi, T., Nakamura, Y., & Toshinawa, T. (1991). Ground motion characteristics in the San Francisco Bay area detected by microtremor measurements. In S. Prakash (Ed.), *Proceedings of the second international conference on recent advances in geotechnical earthquake engineering and soil dynamics* (pp. 1643–1648). St. Louis: University of Missouri.
- Rathod, G.W. (2018a). Seismic ground response analysis and estimation of the seismic wave amplification for Johannesburg region. Council for Geoscience, Report number, 2018-0232.
- Rathod, G.W. (2018b). Seismic ground response analysis and estimation of the seismic wave amplification for KOSH region. Council for Geoscience, Report number, 2018-0233.
- Robb, L. L., Brandl, G., Anhaeusser, C. R., & Poujol, M. (2006). Archaean granitoid intrusions. In M. R. Johnson, C. R. Anhaeusser, & R. J. Thomas (Eds.), *The Geology of South Africa* (pp. 57–94). Pretoria: Geological Society of South Africa, Johannesburg/Council for Geoscience, South Africa.
- Singh, S. K., Lermo, J., Dominguez, T., Ordaz, M., Espinosa, J. M., Mena, E., et al. (1988). The Mexico earthquake of September 19, 1985—a study of seismic waves in the Valley of Mexico with respect to a hill zone site. *Earthquake Spectra*, 4, 653–673.
- Tankard, A. J., Jackson, M. P. A., Erickson, K. A., Hobday, O. K., Hunter, D. R., & Minter, W. E. L. (1982). *Crustal evolution of southern Africa: 3.8 billion years of earth history*. New York: Springer.
- Zaharia, B., Radulian, M., Popa, M., Grecu, B., Bala, A., & Tataru, D. (2008). Estimation of the local response using the Nakamura method for the Bucharesr area. *Romanian Reports in Physics*, 60, 131–144.

(Received January 29, 2018, revised June 5, 2018, accepted July 23, 2018, Published online July 27, 2018)